12-2-2013

Estimating norms of commutators

Terry A. Loring

Freddy Vides

ESTIMATING NORMS OF COMMUTATORS

TERRY A. LORING AND FREDY VIDES

Abstract. We find estimates on the norms commutators of the form $[f(x), y]$ in terms of the norm of $[x, y]$, assuming that x and y are contactions in a C*-algebra $\mathcal{A}$, with x normal and with spectrum within the domain of f. In particular we discuss $\|[x^2, y]\|$ and $\|[x^{1/2}, y]\|$ for $0 \leq x \leq 1$. For larger values of $\delta = \|[x, y]\|$ we can rigorous calculate the best possible upper bound $\|[f(x), y]\| \leq \eta_f(\delta)$ for many f. In other cases we have conducted numerical experiments that strongly suggest that we have in many cases found the correct formula for the best upper bound.

1. Norms of Commutators and functional calculus

In this paper we investigate upper and lower bounds on the norms of commutators in relation to the continuous functional calculus for normal elements of a C^*-algebra. For upper bounds we utilize simple nearby functions to the original function under study, building on a technique introduced by G. K. Pedersen in [11]. For lower bounds, we use Monte Carlo techniques to generate examples.

The only norm we consider on matrices is the operator norm (largest singular value) as this is tied most closely to the norms in C^*-algebras.

Definition 1.1. Suppose Ω is a compact subset of the complex plane and that $f : \Omega \to \mathbb{C}$ is continuous. Define $\eta_f : [0, \infty) \to [0, \infty)$ by

$$\eta_f(\delta) = \sup \left\{ \|[f(X), A]\| \,\middle|\, X, A \in \mathcal{A}, \|A\| \leq 1, \|[X, A]\| = \delta \right\}$$

and the supremum is taken over every possible C^*-algebra $\mathcal{A}$ and taking X and A in $\mathcal{A}$ with X normal with $\sigma(X) \subseteq \Omega$.

A convention is that if $\|[X, A]\| = \delta$ is not possible, we set $\eta_f(\delta) = 0$. We shall see that so long as there is one example where $\|[X, A]\| = \delta$ occurs, whenever $\delta_0 < \delta_1$ we have $\eta_f(\delta_0) \leq \eta_f(\delta)$. Therefore we have an equivalent definition of $\eta_f(\delta)$ if we allow in the supremum all pairs with X normal with spectrum in Ω, the norm of A at most one and $\|[X, A]\| \leq \delta$, so long as $\delta \leq \operatorname{diam}(\Omega)$.

We will focus on two special cases, where Ω is the unit interval or the unit circle.

When $\Omega = [0, 1]$ we are studying the size of $\|[f(X), A]\|$ where $0 \leq X \leq 1$ and A has norm at most one, in any C^*-algebra. Following the arguments used in [10, Corollary 5.4] we can prove the following.

Lemma 1.2. *If $f : [0, 1] \to \mathbb{C}$ is continuous then*

$$\eta_f(\delta) = \sup \left\{ \|[f(X), A]\| \,\middle|\, X, A \in \mathbf{M}_n(\mathbb{C}), 0 \leq X \leq 1, \|A\| \leq 1 \right\}$$

the supremum taken over all n.

2010 *Mathematics Subject Classification.* 47B47, 47A56, 47A58.

Key words and phrases. Commutators, function approximation, functional calculus, normal operators, almost commuting matrices.

The analogous result for the circle is very likely true. In that case, we are working with a unitary U and a contraction A with $\|[U,A]\|$ a specific value. If only we could suppose that A was also unitary, then we could use the fact that the soft torus is residually finite dimensional [6].

Functions on the circle are traditionally studied in the form of periodic functions on the line. In order to be able to use standard notation from Fourier series, we adopt a convention that allows us to apply such a function to a unitary matrix or operator.

For f a continuous function on $\mathbb{R}$ that is periodic, period 2π always assumed, we adopt the notation

$$f[U] = \tilde{f}(U)$$

for U any unitary element in a unital C^*-algebra $\mathcal{A}$, where

$$\tilde{f}(z) = f\left(-i\log(z)\right)$$

for z of modulus one. For example

$$\cos[U] = \tfrac{1}{2}U^* + \tfrac{1}{2}U.$$

Using this notation, we can describe $\eta_{\tilde{f}}$ as the smallest function on $[0,\infty)$ such that

$$U^*U = UU^* = I \text{ and } \|A\| \leq 1 \implies \|[f[U],A]\| \leq \eta_{\tilde{f}}\left(\|[U,A]\|\right).$$

It is trivial to prove that when an element A in $\mathcal{A}$ commutes with U then A commutes with $f[U]$. What we seek are good estimates that quantify the statement that when A almost commutes with U then it also almost commutes with $f[U]$.

It is important to mention that the estimates obtained in this paper can be applied to arbitrary derivations in the C*-algebra $\mathcal{A}$.

As to functions f that are periodic, we need

$$\|f\|_\infty = \sup_{-\pi\leq x\leq\pi} |f(x)|$$

and, whenever f has Fourier series converging absolutely, we use

$$\|f\|_{\mathcal{F}} = \|\hat{f}\|_1$$

the ℓ^1 norm of the Fourier series.

Example 1.3. Let $f(x) = \cos(x)$. Assuming U is unitary and A has norm at most one,

$$\begin{aligned}\|[f[U],A]\| &= \frac{1}{2}\|[U^*,A] + [U,A]\| \\ &\leq \frac{1}{2}\|[U^*,A]\| + \frac{1}{2}\|[U,A]\| \\ &= \|[U,A]\|\end{aligned}$$

so $\eta_{\tilde{f}}(\delta) \leq \delta$. To find a lower bound, we use

$$U = \begin{bmatrix} 1 & 0 \\ 0 & -1 \end{bmatrix}$$

and

$$A = \begin{bmatrix} 0 & t \\ t & 0 \end{bmatrix}$$

so that

$$\|[U,A]\| = \left\| \begin{bmatrix} 0 & t \\ -t & 0 \end{bmatrix} - \begin{bmatrix} 0 & -t \\ t & 0 \end{bmatrix} \right\| = \left\| \begin{bmatrix} 0 & 2t \\ -2t & 0 \end{bmatrix} \right\| = 2t$$

and since $f[U] = U$,

$$\eta_{\tilde{f}}(\delta) = \delta$$

for all δ in $[0,2]$. For larger δ we have $\eta_{\tilde{f}}(\delta)$ equal to zero.

This is about the only example where we know η_f exactly for all δ. However, we can compute $\eta_f(\delta)$ exactly for larger values of δ for many f.

There is a general trend where results about commutators are related to continuity results involving the functional calculus. See [3], for example. In the case of unitaries there is an easy connection between the two topics.

Lemma 1.4. *For f that is continuous and periodic, if V and V_1 are unitaries then*

$$\|f[V] - f[V_1]\| \leq \eta_{\tilde{f}}\left(\|V - V_1\|\right).$$

Proof. Notice

$$\left\| \left[\begin{pmatrix} 0 & 1 \\ 1 & 0 \end{pmatrix}, \begin{pmatrix} V & 0 \\ 0 & V_1 \end{pmatrix} \right] \right\| = \|V - V_1\|$$

and

$$\left\| \left[\begin{pmatrix} 0 & 1 \\ 1 & 0 \end{pmatrix}, f\left[\begin{pmatrix} V & 0 \\ 0 & V_1 \end{pmatrix} \right] \right] \right\| = \|f[V] - f[V_1]\|$$

so this is an easy calculation. □

2. Upper bounds

The following generalizes a trick in Pedersen's work on commutators and square roots, [11, Lemma 6.2].

Lemma 2.1. *Suppose f, g and h are continuous and periodic, that g' has absolutely convergent Fourier series. If $f = g + h$ then*

$$\eta_{\tilde{f}}(\delta) \leq m\delta + b$$

where $m = \|g'\|_{\mathcal{F}}$ and

$$b = 2 \min_{\lambda \in \mathbb{C}} \|h - \lambda\|_{\infty}.$$

When h is real valued then $b = \max(h) - \min(h)$.

Remark 2.2. *In the special case where $h = 0$ we recover the folk theorem that says*

$$\|[g[V], A]\| \leq \|g'\|_{\mathcal{F}} \|[V, A]\| \tag{2.1}$$

for any unitary V and any operator A, now without norm restriction because the two sides are homogeneous in A. For related estimates, see [1, §5].

Proof. Suppose $\|A\| \leq 1$ and V is unitary. Since

$$\|[f[V], A]\| \leq \|[g[V], A]\| + \|[h[V], A]\|$$

and

$$\|[h[V], A]\| = \|[h[V] + \lambda I, A]\| = \|[(h + \lambda)[V], A]\|$$

it suffices to prove equation (2.1) and

$$\|[h[V], A]\| \leq 2 \|h\|_\infty . \tag{2.2}$$

We know

$$g(x) = \sum_{n=-\infty}^{\infty} a_n e^{inx}$$

where $\sum |na_n| < \infty$ and so

$$\begin{aligned} \|[g[V], A]\| &= \left\| \left[\sum_{n=-\infty}^{\infty} a_n V^n, A \right] \right\| \\ &\leq \sum_{n=-\infty}^{\infty} |a_n| \, \|[V^n, A]\| \\ &\leq \sum_{n=-\infty}^{\infty} |na_n| \, \|[V, A]\| \\ &= \|g'\|_{\mathcal{F}} \, \|[V, A]\| . \end{aligned}$$

The spectral theorem tells us $\|h[V]\| \leq \|h\|_\infty$ and so

$$\|[h[V], A]\| = \|h[V]A - Ah[V]\| \leq 2 \|h[V]\| \, \|A\| \leq 2 \|h\|_\infty .$$

□

A similar result holds for the unit interval. We use polynomials and power series to the nicer approximating functions. We could also use functions with nice Fourier transforms. As we are interested in machine generated proofs, polynomials are easiest to explore as they have a nice countable basis.

Lemma 2.3. *Suppose f, g and h are continuous on $[0, 1]$ and that g is analytic, with power series*

$$g(x) = \sum_{n=0}^{\infty} a_n x^n.$$

If $f = g + h$ then

$$\eta_f(\delta) \leq m\delta + b$$

where

$$m = \sum_{n=0}^{\infty} |na_n|$$

and

$$b = 2 \min_{\lambda \in \mathbb{C}} \|h - \lambda\|_\infty .$$

Proof. We know $\sum |na_n| < \infty$ and so

$$\begin{aligned}\|[g(H), A]\| &= \left\| \left[\sum_{n=0}^{\infty} a_n H^n, A \right] \right\| \\ &= \left\| \sum_{n=0}^{\infty} a_n \left[H^n, A \right] \right\| \\ &\leq \sum_{n=0}^{\infty} |a_n| \, \|[H^n, A]\| \\ &\leq \sum_{n=0}^{\infty} |na_n| \, \|[H, A]\| \, .\end{aligned}$$

□

Remark 2.4. *The lemma 2.3 holds modified mutatis mutandis for continuous functions on* $-1 \leq H \leq 1$.

Remark 2.5. *From* [13, Corollary 2.5.4] *we have that any derivation* δ *in a C*-Algebra* A *on a Hilbert space* H*, can be written as* $\delta(a) := [x, a]$*, for a fixed* $x \in \overline{A}^{weak}$ *in* $B(H)$*, and any* $a \in A$*. Hence we will have that the previous inequalities for commutators hold for derivations in C*-Algebras.*

3. Lower bounds

We must look at examples to produce lower bounds. Fortunately, a single example tells us something about $\eta_f(\delta)$ for all values of δ.

Lemma 3.1. *Suppose* $f : \Omega \to \mathbb{C}$ *is continuous. If* $\delta = \|[X, A]\|$ *for* X *normal and* A *of norm at most one then*

$$0 \leq t \leq 1 \implies \eta_f(t\delta) \geq t\|[f(X), A]\|.$$

and

$$\delta \leq \delta_1 \leq \operatorname{diam}(\Omega) \implies \eta_f(\delta_1) \geq \|[f(X), A]\|.$$

Proof. For the first implication, consider the pair X, tA.

Since δ_1 is less the the diameter of Ω, there are x_1 and x_2 in Ω distance δ_1 apart. The commutator of

$$A_1 = \begin{pmatrix} 0 & 1 \\ 1 & 0 \end{pmatrix}$$

with

$$X_1 = \begin{pmatrix} \omega_1 & 0 \\ 0 & \omega_2 \end{pmatrix}$$

has norm δ_1. Now we use $X \oplus X_1$ and $A \oplus A_1$ to prove the inequality. Here it is essential that we are using the operator norm so that

$$\|[X \oplus X_1, A \oplus A_1]\| = \|[X, A] \oplus [X_1, A_1]\| = \max(\|[X, A]\|, \|[X_1, A_1]\|)$$

etc. □

Lemma 3.2. *Suppose $f : \Omega \to \mathbb{C}$ is continuous. If $0 \leq \delta \leq \operatorname{diam}(\Omega)$ then $\eta_f(\delta) \geq \lambda_f(\delta)$ where λ_f is the function on $[0, \infty)$ defined by*

$$\lambda_f(\delta) = \max\left\{ |f(x_2) - f(x_1)| \;\middle|\; |x_2 - x_1| \leq \delta \right\}.$$

Proof. The follows easily from examining X_1 and A_1 as defined in the preceding proof. □

Remark 3.3. *If f is periodic and continuous then*

$$\lambda_{\tilde{f}}(\delta) = \max\left\{ |f(x_2) - f(x_1)| \;\middle|\; |x_2 - x_1| \leq 2\arcsin\left(\tfrac{\delta}{2}\right) \right\}.$$

Kato shows that $f(x) = |x|$ is not operator Lipshitz using explicit examples. Beyond this, and the basic examples above, we find no explicit examples in the literature making $\|[f(X), A]\|$ large.

We turn to Monte Carlo methods to find examples. This is more difficult than it might appear, as the norms of commutators of "random matrices" have behavior that is too predictable. This was proven the case for the Frobenious norm in [4]. We find experimentally that the obvious methods to generate random numerical examples fail miserably.

By using a non-standard matrix ensembles, and a lot of computer time, we are able to get an idea of what η_f looks like.

A different approach to creating lower bounds is taken by Aleksandrov and Peller. For example, they derive a lower bounds on $\||X| - |Y|\|$ such as [2, Theorem 6.6]. This lower bound determines asymptotic behavior but is not full explicit as it involves an unknown constant.

4. Conjectures

It is not clear who first asserted the following, but it appears in [12].

Conjecture 4.1.

$$\left\| \left[X^{\frac{1}{2}}, A \right] \right\| \leq \|[X, A]\|^{\frac{1}{2}}$$

wherever $0 \leq X \leq 1$ and $\|A\| \leq 1$.

This is equivalent to the assertion that if $f(x) = \sqrt{x}$ then

$$\eta_f(\delta) = \delta^{\frac{1}{2}}$$

for $0 \leq \delta \leq \operatorname{diam}(\Omega)$.

Pedersen [12] attacks this conjecture using polynomial approximation. A limitation of this method is that we don't really know η_p for a polynomial, not even for $p(x) = x^2$.

Conjecture 4.2. *For $p(x) = x^2$ defined on $[0, 1]$ we have $\gamma_p(\delta) = 2\delta - \delta^2$. Equivalently*

$$\left\| \left[X^2, A \right] \right\| \leq 2\|[X, A]\| - \|[X, A]\|^2$$

wherever $0 \leq X \leq 1$ and $\|A\| \leq 1$.

The numerical evidence points to η_f being concave for all continuous f. For really poorly behaved f it is possible that the numerical evidence is misleading. Our experiments worked only with real-valued functions, just to limit the scope. Perhaps for real polynomials we know the answer.

Conjecture 4.3. *If p is a real polynomial, considered as a function on $[0, 1]$ then γ_p is the smallest concave and non-decreasing function on $[0, 1]$ that is greater than or equal to λ_f.*

Polynomials on the circle, with real coefficients, were almost as easy to investigate.

Conjecture 4.4. *If p is a real polynomial, considered as a function on the unit circle, then γ_p is the smallest concave and non-decreasing function on $[0,2]$ that is greater than or equal to λ_f.*

5. The square root

For any a greater than 0 and at most 1 let g be the Taylor expansion of f at a,

$$g(x) = \frac{1}{2\sqrt{a}}(x-a) + \sqrt{a}.$$

and $h = f - g$,

$$h(x) = \sqrt{x} - \frac{1}{2\sqrt{a}}(x-a) - \sqrt{a}.$$

Clearly $\max(h) = h(a) = 0$ and the minimum occurs at either $x = 0$ or $x = 1$, where the values are

$$h(0) = -\tfrac{1}{2}\sqrt{a}$$

and

$$h(1) = 1 - \frac{1}{2\sqrt{a}} - \frac{\sqrt{a}}{2}.$$

For $\frac{1}{4} \leq a \leq 1$ we find

$$\min(h) = -\tfrac{1}{2}\sqrt{a}.$$

Therefore,

$$\eta_f(\delta) \leq \frac{1}{2\sqrt{a}}\delta + \tfrac{1}{2}\sqrt{a} \tag{5.1}$$

for $\frac{1}{4} \leq a \leq 1$, which is very interesting since at $\delta = a$ the right hand side is $\sqrt{a}$. We have proven a special case of the conjecture, which we state as a lemma.

Lemma 5.1. *When $0 \leq H \leq 1$ and $\|A\| \leq 1$ and we have*

$$\|[H,A]\| \geq \frac{1}{4} \implies \left\| \left[H^{\frac{1}{2}}, A \right] \right\| \leq \|[H,A]\|^{\frac{1}{2}}.$$

Pedersen uses the following easy lemma.

Lemma 5.2. *If f_1 is continuous on $[0,1]$ and we set*

$$f_2(x) = 1 - f_1(1-x)$$

then $\gamma_{f_1} = \gamma_{f_2}$.

His proof of the inequality

$$\left\| \left[H^{\frac{1}{2}}, A \right] \right\| \leq \frac{2}{\sqrt{\pi}} \|[H,A]\|^{\frac{1}{2}} \tag{5.2}$$

(notice $2\pi^{\frac{1}{2}} \approx 1.128$) in [11, Lemma 6.2] invokes Lemma 2.3 infinitely many times, as g ranges over the Taylor polynomials for $f(x) = 1 - \sqrt{1-x}$ expanded at 0. While (5.2) is the statement

$$\gamma_f(\delta) \leq \frac{2}{\sqrt{\pi}}\delta^{\frac{1}{2}}$$

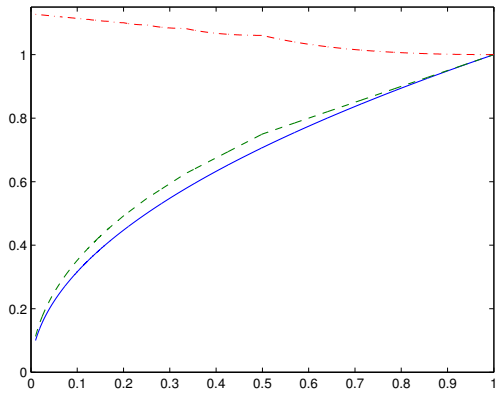

FIGURE 5.1. Bound on $\left\| \left[H^{\frac{1}{2}}, A \right] \right\|$ for varying values of $\|[H, A]\|$ as found by Pedersen, shown as a dashed line. The solid curve is $\sqrt{\delta}$. The top curve is the ratio of the bound to $\sqrt{\delta}$.

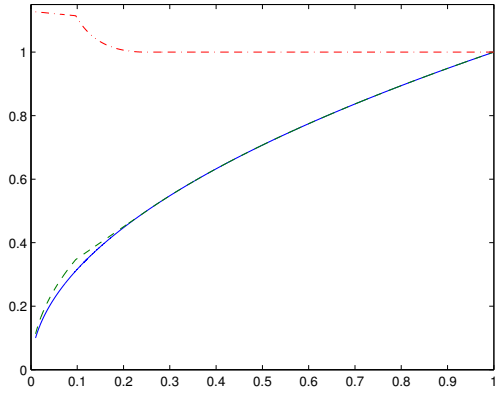

FIGURE 5.2. Bound on $\left\| \left[H^{\frac{1}{2}}, A \right] \right\|$ for varying values of $\delta = \|[H, A]\|$ as improved by the inequalities (5.1). The solid curve is $\sqrt{\delta}$. The dashed curve is the upper bound $\gamma_0(\delta)$ of Theorem 5.3. The top curve is $\gamma_0(\delta)/\sqrt{\delta}$.

what he actually proves is a bound that is significantly smaller for δ close to 1. Indeed, he showed γ_f to be bounded by the function shown in Figure 5.1

The minimum of all these lines does not lead to an easy formula, so we state our best theorem regarding the square root in terms on a plotted function.

Theorem 5.3. *If* $0 \leq H \leq 1$ *and* $\|A\| \leq 1$ *then*

$$\left\| \left[H^{\frac{1}{2}}, A \right] \right\| \leq \gamma_0 \left(\|[H, A]\| \right)$$

where γ_0 *is the function illustrated in Figure 5.2.*

Proof. We simply combine all the linear bounds in [11, Lemma 6.2] with Lemma 5.1. □

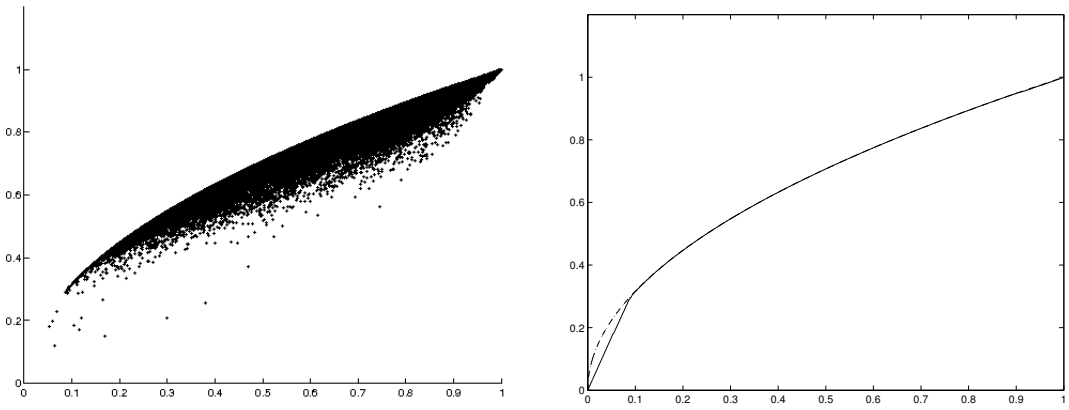

FIGURE 5.3. $f(x) = \sqrt{x}$ and $n = 4$. Approximately 10,000,000 pairs were tested, with 120,888 pairs computed precisely.

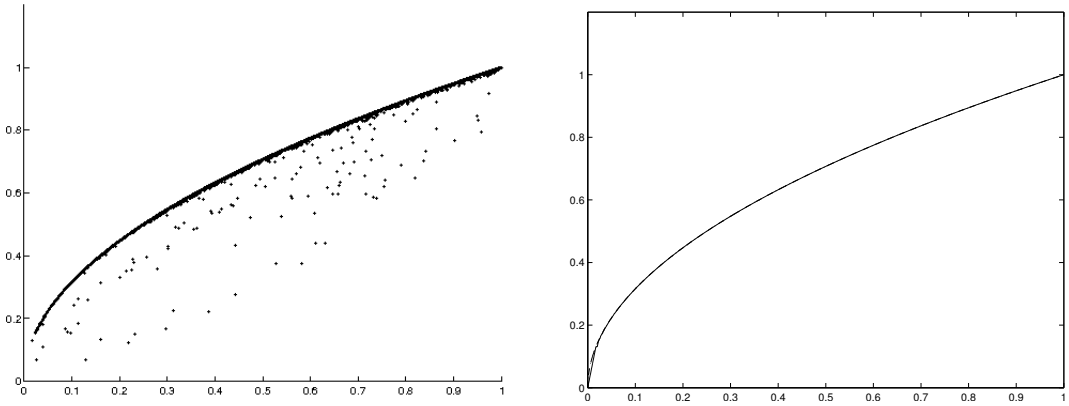

FIGURE 5.4. $f(x) = \sqrt{x}$ and $n = 256$. Approximately 10,000,000 pairs were tested, with 29,642 pairs computed precisely.

We present some of our numerical evidence supporting Conjecture 4.2 in Figures 5.3 and 5.4.

6. A few polynomials

We conjecture that η_f is concave at least in the case where f is a real polynomial.

Example 6.1. For $f(x) = x^2$ on $[0, 1]$ the numerical evidence is compelling. Some of our evidence is in Figures 6.1 and 6.2.

If we apply Lemma 2.3 with $g(x) = ax$ for some $0 \leq a \leq 1$, we easily establish that $\eta_f(\delta_a) = 2\delta_a - \delta_a^2$ where $\delta_a = 1 - a/2$. That is, we have proven that for $0 \leq X \leq 1$ and $\|A\| \leq 1$,

$$\|[X, A]\| \geq \frac{1}{2} \implies \left\|\left[X^2, A\right]\right\| \leq 2\,\|[X, A]\| - \|[X, A]\|^2\,. \tag{6.1}$$

Now we consider a polynomial where λ_f is not concave, specifically $f(x) = (x - 0.5)^3 + x$. We start with some rigorous upper bounds.

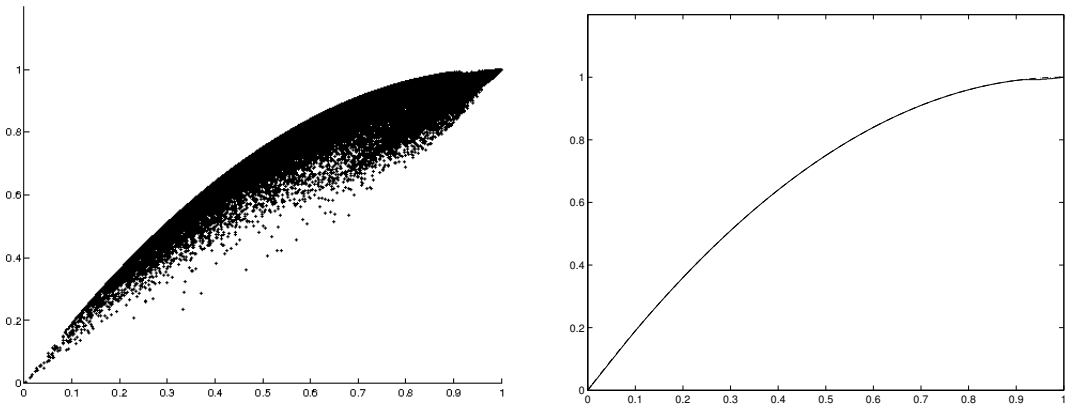

FIGURE 6.1. $f(x) = x^2$ and $n = 4$. Approximately 10,000,000 pairs were tested, with 120,760 pairs computed precisely.

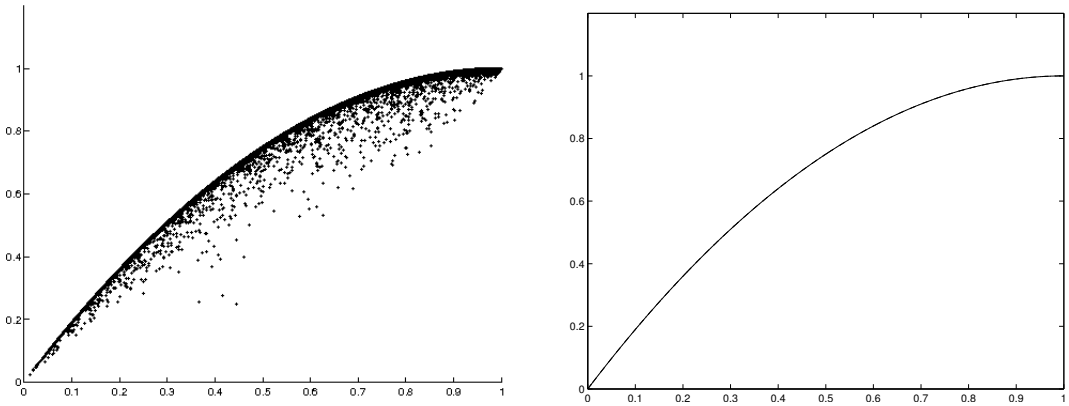

FIGURE 6.2. $f(x) = x^2$ and $n = 64$. Approximately 10,000,000 pairs were tested, with 102,677 pairs computed precisely.

Theorem 6.2. *Let $f(x) = (x - 0.5)^3 + x$, considered as a function on $[0, 1]$. Then*

$$\eta_f(\delta) \leq \frac{7}{4}\delta$$

and

$$\eta_f(\delta) \leq \frac{19}{16}\delta + \frac{1}{16}$$

Proof. The first assertion follows from the fact that $f'(1) = \frac{7}{4}$. For the second, we just apply Lemma 2.3 with $g = \frac{19}{16}x$. These two upper bounds are shown in Figure 6.3 □

These two upper bounds are shown in Figure 6.3. The numerical evidence here required more computing time than the previous examples, as we needed to examine over a billion pairs before a pattern become apparent. Our Monte Carlo method struggles when λ_f is not concave. Evidence supporting our conjecture for this polynomial is presented in Figures 6.4-6.6

Finally, we give in Figures 6.7 and 6.8 numerical evidence for our conjecture for a polynomial with positive coefficients.

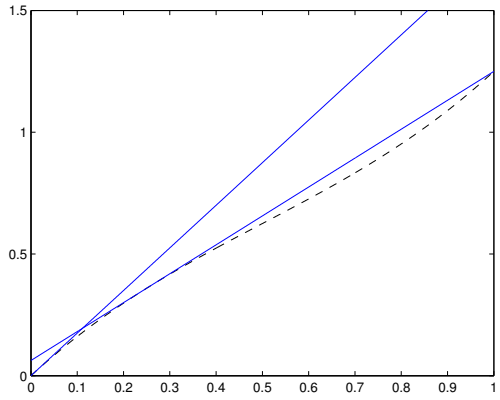

FIGURE 6.3. $f(x) = \left(x - \frac{1}{2}\right)^3 + x$ with the rigorous upper bounds plotted. The dotted line is λ_f.

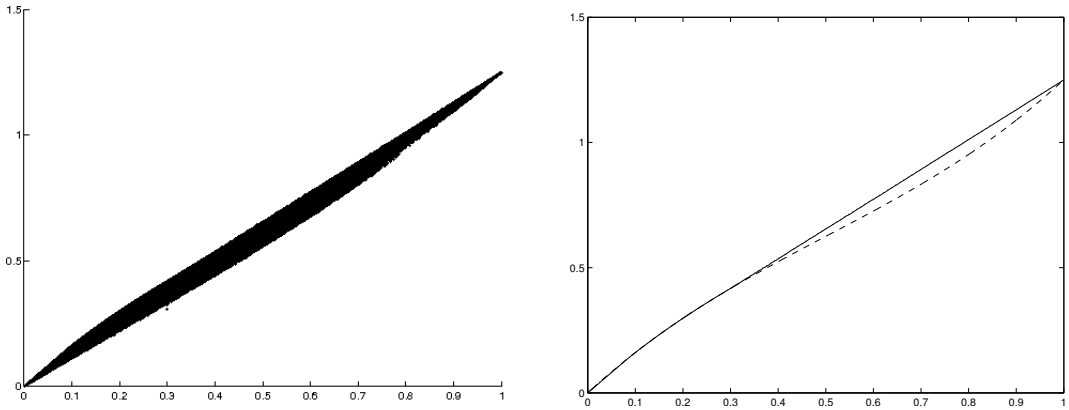

FIGURE 6.4. $f(x) = (x - 0.5)^3 + x$ and $n = 4$. Approximately 500,000,000 pairs were tested, of which 3,995,117 were computed precisely and plotted.

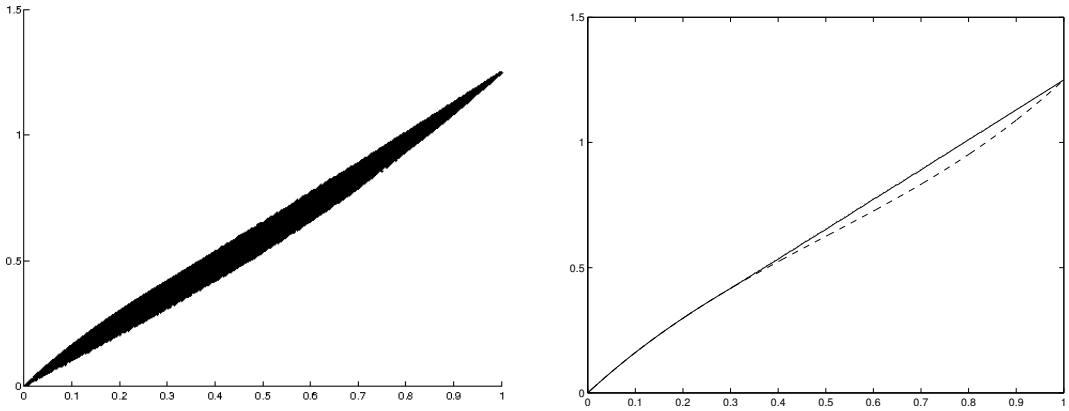

FIGURE 6.5. $f(x) = (x - 0.5)^3 + x$ and $n = 8$. Approximately 500,000,000 pairs were tested, of which 4,590,893 were computed precisely and plotted.

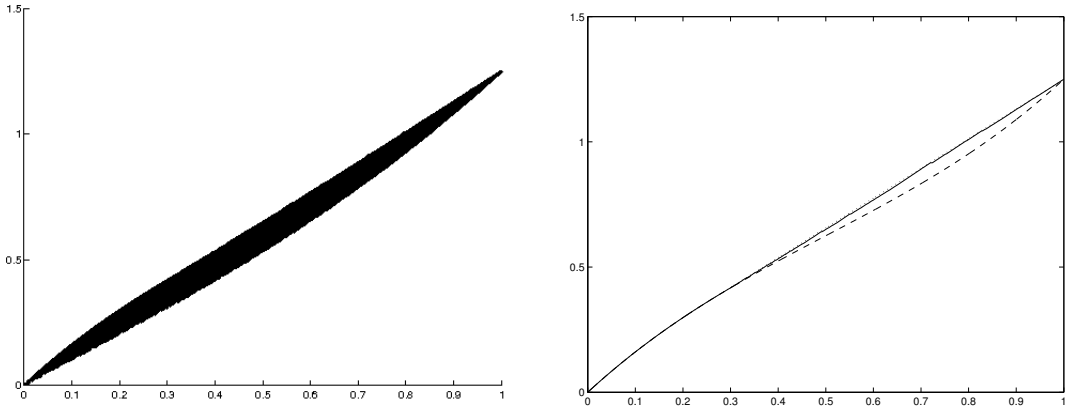

FIGURE 6.6. $f(x) = (x - 0.5)^3 + x$ and $n = 16$. Approximately 500,000,000 pairs were tested, of which 3,538,440 were computed precisely and plotted.

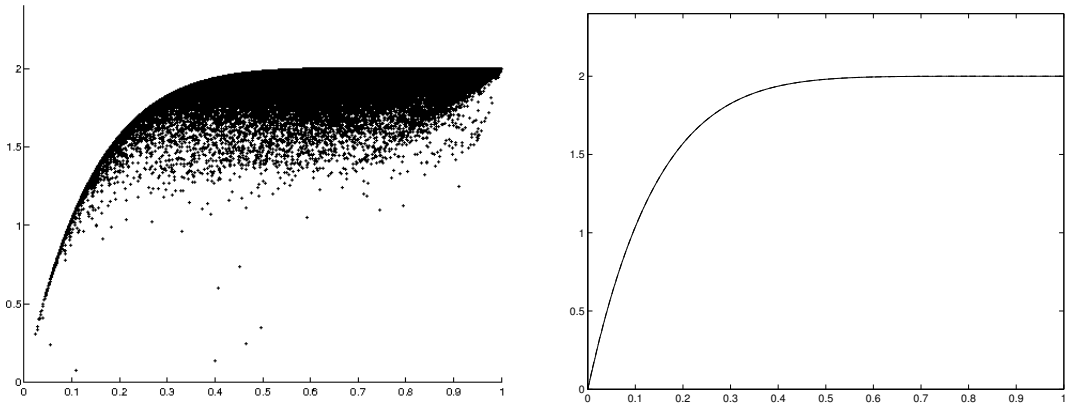

FIGURE 6.7. $f(x) = x^8 + x^6$ and $n = 8$. Approximately 10,000,000 pairs were tested, with 235,201 pairs computed precisely.

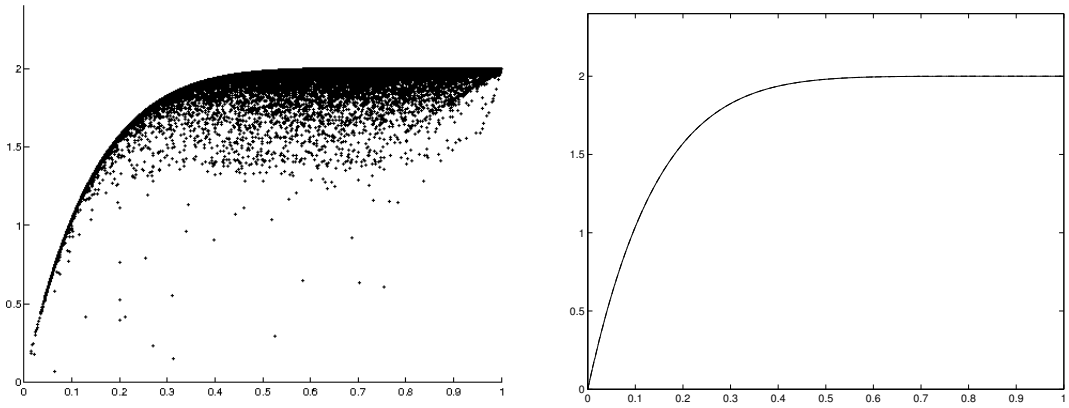

FIGURE 6.8. $f(x) = x^8 + x^6$ and $n = 16$. Approximately 10,000,000 pairs were tested, with 264967 pairs computed precisely.

7. Examples of operator functions of a unitary

The impetus for finding quantitative bounds on $\|[f(X), A]\|$ for larger values of $\delta = \|[X, A]\|$ was the computationally challenges in studying disordered systems [8]. The Bott index (and related indices) for almost commuting matrices need to be compute efficiently. The Bott index is an integer that determines if a given pair of almost commuting unitary matrices is close to a commuting pair of matrices.

Our formulas for the Bott index apply to unitary matrices triples of functions

$$f, g, h : \mathbb{T}^2 \to \mathbb{R}^3$$

with certain topological properties. Our choice of examples in this section is partially driven by the desire to understand formulas for the Bott index, but we also chose examples that explain our conjecture that $\eta_{\tilde{f}}$ is convex for all triginometric polynomials.

Corollary 7.1. *If f has uniformly convergent Fourier series,*

$$f(x) = \sum_{n=-\infty}^{\infty} a_n e^{inx}$$

then

$$\eta_{\tilde{f}}(\delta) \leq 2 \sum_{n=-\infty}^{\infty} |a_n|.$$

and

$$\eta_f(\delta) \leq \delta \sum_{n=-N}^{N} |n a_n| + 2 \sum_{n=N+1}^{\infty} \left(|a_n| + |a_{-n}|\right). \tag{7.1}$$

Proof. If we take

$$g(x) = \sum_{n=-N}^{N} a_n e^{inx}$$

and apply Lemma 2.1 we obtain (7.1). For the other we set g to 0. □

Example 7.2. Consider the triangle wave

$$f(x) = \begin{cases} 1 + \frac{2}{\pi} x & -\pi \leq x \leq 0 \\ 1 - \frac{2}{\pi} x & 0 \leq x \leq \pi \end{cases}$$

we have $a_{2n} = 0$ and

$$a_{2n-1} = \frac{8}{\pi^2} \frac{1}{(2n-1)^2}.$$

Using Corollary 7.1 we get the bound on $\eta_{\tilde{f}}$ as indicated in Figure 7.1. Slightly better estimates are possible if we exactly compute the min and max of the difference between f and its trigonometric polynomial approximations. We could also eliminate the corners by interpolating with trig polynomials between the truncated Fourier series.

The triangle wave is, up to scaling, the function used in [7] as one of the functions defining the Bott invariant. It is only by Monte Carlo methods that we get an idea what $\eta_{\tilde{f}}$ looks like, and it is definitely larger than what we get from making λ_f concave. This example is why we are limiting Conjecture 4.4. Our numerical examples for the triangle wave are shown in Figures 7.2 and 7.3.

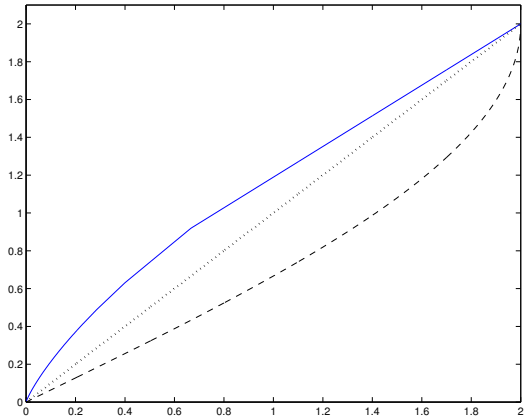

FIGURE 7.1. Bounds on $\|[f[V], A]\|$ for varying values of $\delta = \|[V, A]\|$ for f a triangle wave. The solid line is a proven upper bound. The dashed line is the lower bound $\lambda_{\tilde{f}}$. The smallest convex nondecreasing function larger than $\lambda_{\tilde{f}}$ is shown as a dotted line.

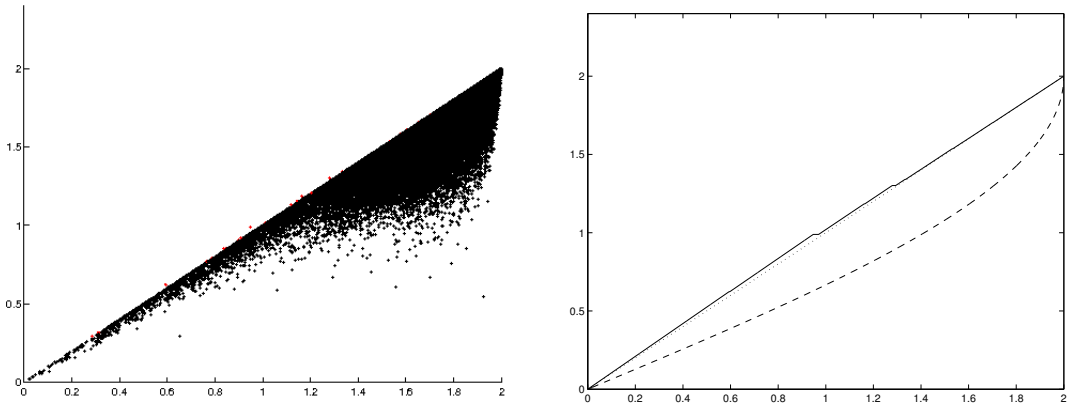

FIGURE 7.2. f a triangle wave on the circle and $n = 4$. Approximately 250,000,00 pairs were tested, with 144,732 pairs computed precisely.

Of course the graphs should be rising, and yet they are falling. This is a short-coming of our Monte Carlo method. Presumably there is a better distribution to use in creating examples.

The companion functions g and h in the Bott index definition from [7] are not so well behaved. We consider only h as g is just a translation. The function h we now examine.

Example 7.3. The function h used in [7] is

$$h(x) = \begin{cases} \sqrt{1 - \frac{4}{\pi^2}x^2} & \text{if } x \in \left[-\frac{\pi}{2}, \frac{\pi}{2}\right] \\ 0 & \text{if } x \notin \left[-\frac{\pi}{2}, \frac{\pi}{2}\right] \end{cases} \tag{7.2}$$

and $\eta_{\tilde{h}}$ tends to zero rather slowly. The lower bound $\lambda_{\tilde{h}}$ from Lemma 3.2 is shown in Figure 7.4.

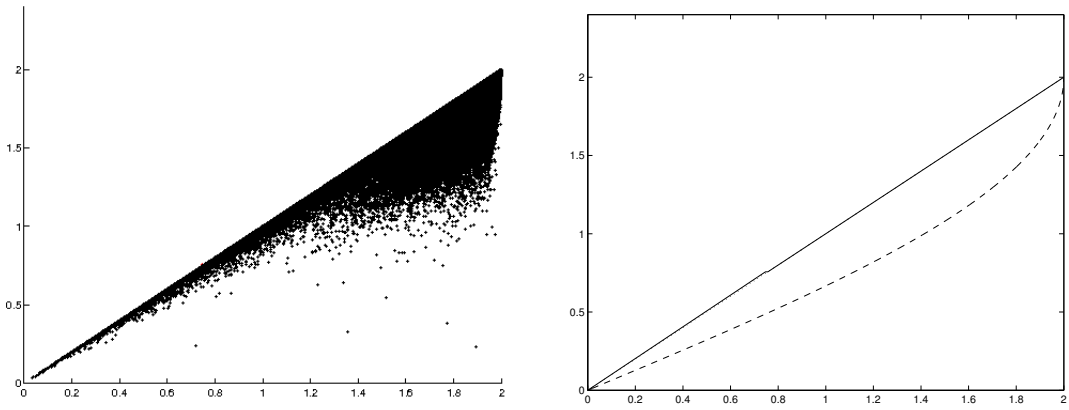

FIGURE 7.3. f a triangle wave on the circle and $n = 8$. Approximately 250,000,00 pairs were tested, with 182,481 pairs computed precisely.

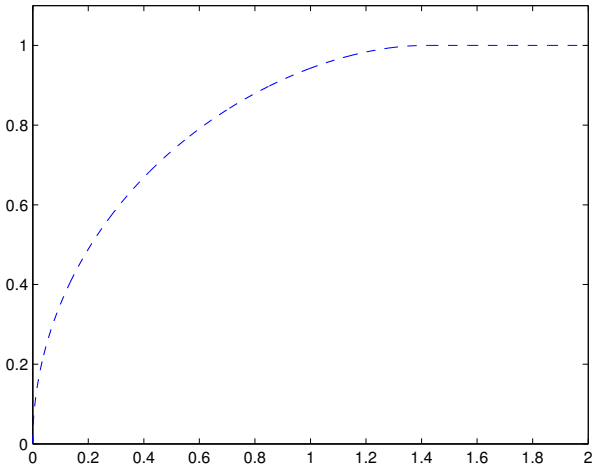

FIGURE 7.4. A lower bound on $\|[h[V], A]\|$ where h is the bump function on the circle defined in Equation 7.2.

Example 7.4. Let

$$f(x) = 8\sin(x) + \sin(4x).$$

Using Lemma 2.1 with $g = f$ and then with $g = 8\sin(x)$ we discover upper-bounds $12x$ and $8x + 2$. These come very close to $\lambda_{\tilde{f}}$ overall and essentially equal to it for δ in $[0.8, 2]$, as shown in Figure 7.5. The results of computing a quarter billion examples of 4-by-4 and 8-by-8 matrices are shown in Figures 7.6 and 7.7.

Example 7.5. Let

$$f(x) = (1/128)\left(150\sin(x) + 25\sin(3x) + 3\sin(5x)\right).$$

This is the replacement for the triangle wave we use in [8] for a fast method of calulating the Bott index. The numerical evidence that our conjecture holds here is shown in Figures 7.8 and 7.9.

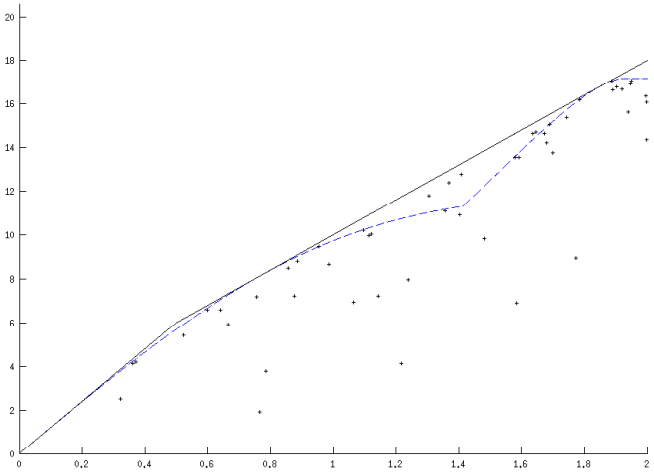

FIGURE 7.5. $f(x) = 8\sin(x) + \sin(4x)$ and $n = 64$. Approximately 1,000 pairs were tested, with pairs computed precisely. The rigorous upper bound $\max(12x, 8x + 2)$ is shown using solid lines.

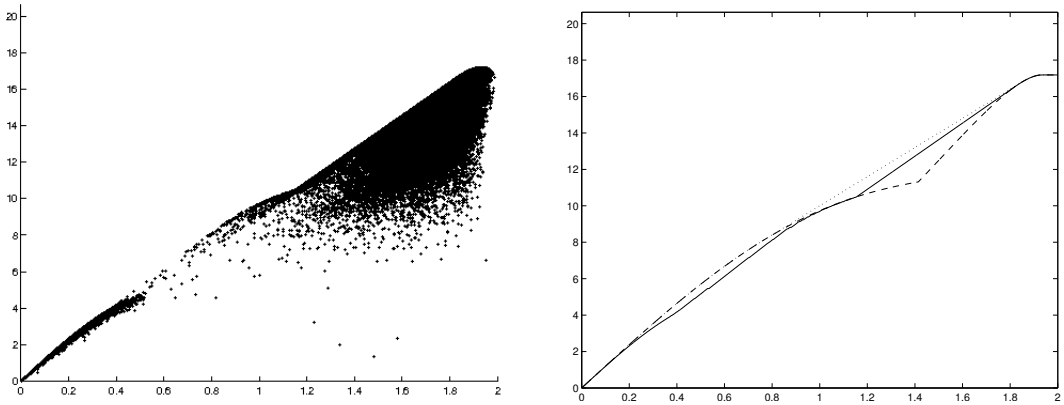

FIGURE 7.6. $f(x) = 8\sin(x) + \sin(4x)$ and $n = 4$. Approximately 250,000,000 pairs were tested, with 98,719 pairs computed precisely.

8. The absolute value of hermitian operators

In this section we will consider the function $f(x) := |x|$ and $X, Y \in \mathcal{A}$, such that $-1 \leq X \leq 1$, $\|Y\| \leq 1$, because of the inequality

$$\|[X^2, Y]\| \leq 2\|[X, Y]\|$$

we get a first estimate of the form

$$\begin{aligned} \|[|X|, Y]\| &\leq \frac{2}{\sqrt{\pi}}\|[X^2, Y]\|^{1/2} \\ &\leq 2\sqrt{\frac{2}{\pi}}\|[X, Y]\|^{1/2}. \end{aligned}$$

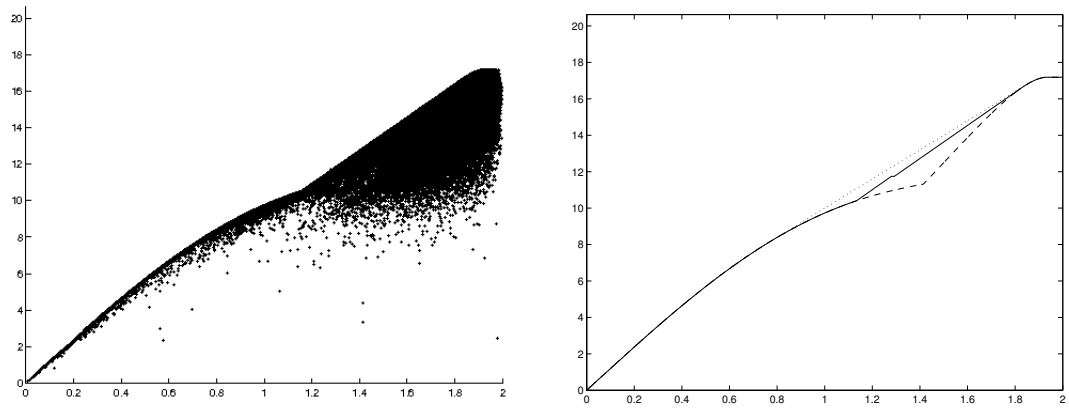

FIGURE 7.7. $f(x) = 8\sin(x) + \sin(4x)$ and $n = 8$. Approximately 250,000,000 pairs were tested, with 214,218 pairs computed precisely.

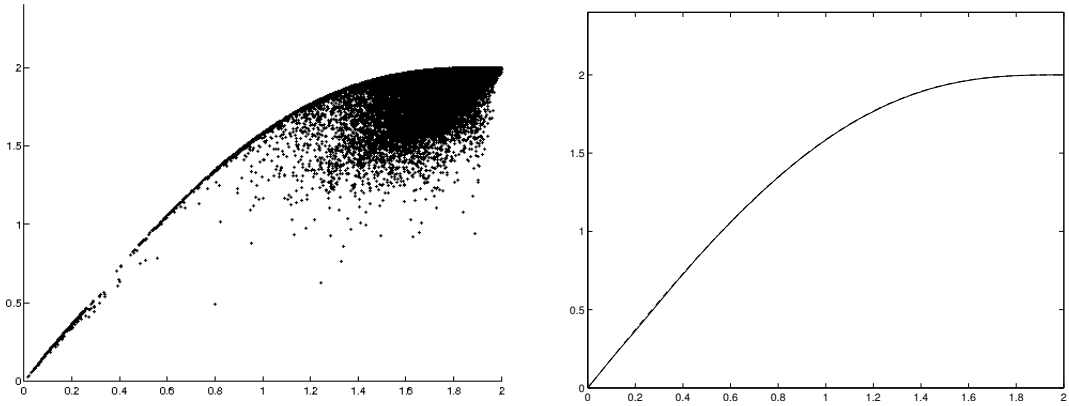

FIGURE 7.8. $f(x) = (1/128)\,(150\sin(x) + 25\sin(3x) + 3\sin(5x))$ and $n = 4$. Approximately 10,000,000 pairs were tested, with 28,168 pairs computed precisely.

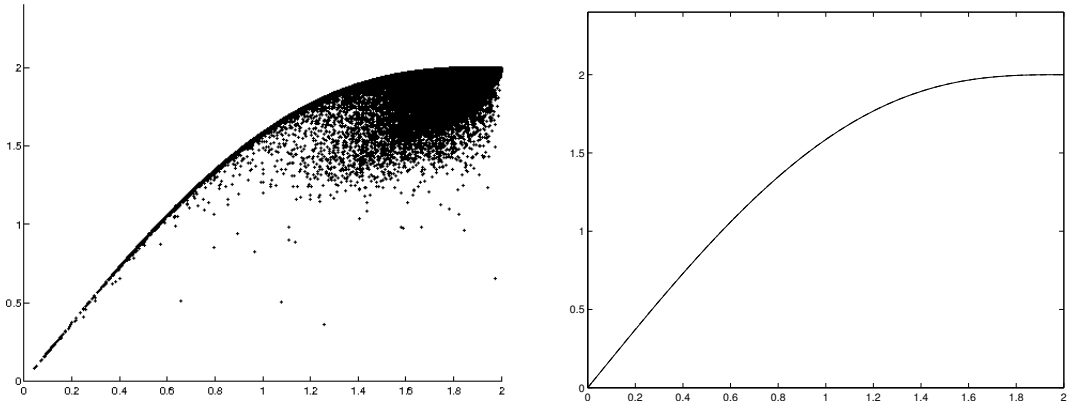

FIGURE 7.9. $f(x) = (1/128)\,(150\sin(x) + 25\sin(3x) + 3\sin(5x))$ and $n = 8$. Approximately 10,000,000 pairs were tested, with 105,724 pairs computed precisely.

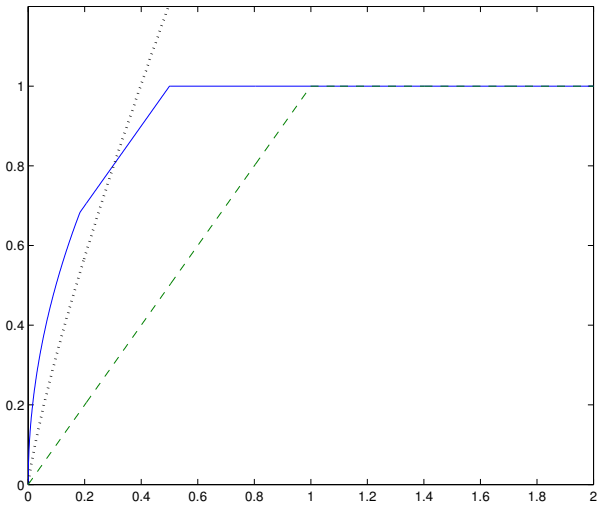

FIGURE 8.1. Bounds on $\|[|X|, Y]\|$ in terms of $[X, Y]$. The dashed line is the lower bound from our basic estimate. The solid line is the upper bound we have proven. The dotted line is an estimate by Kato [9].

Theorem 8.1. *Let $f(x) = |x|$, considered as a function on $[0, 1]$. The function η_f is bounded above by*

$$\max\left(2\sqrt{\frac{2}{\pi}}\delta^{\frac{1}{2}}, \frac{1}{2} + \delta, 1\right).$$

Proof. We have already proven that 1 and $2\sqrt{\frac{2}{\pi}}\delta^{\frac{1}{2}}$ are upper bounds. The bound $\lambda(\delta) \leq \frac{1}{2} + \delta$ follows from Remark 2.4 if we break up $f(x) = |x|$ into $f = g + h$ with

$$g(x) = \frac{1}{2}x^2.$$

$$h(x) = |x| - \frac{1}{2}x^2.$$

Then $\lambda(\delta) \leq m\delta + b$ where $m = 1$ and

$$b = \max_{-1\leq x\leq 1}(h(x)) - \min_{-1\leq x\leq 1}(h(x)) = \frac{1}{2}.$$

□

To put this in context, Kato [9] (see also [5]) obtains the upper bound $\frac{2}{\pi}\delta\ln(2 + 2\delta^{-1})$.

The numerical evidence here was derived using $f(x) = |x - 1/2|$ on $[0, 1]$ so that we could utilize the code used in the earlier examples. Thus the data in Figures 8.2-8.4 needs to be scaled by 2 in both directions to apply to the absolute value on $[-1, 1]$.

9. Monte Carlo Methods

Our algorithms, for the case of f on $[0, 1]$, generate examples by an ad-hoc method. A fast approximation is done for $\|[X, A]\|$ and $\|[f(X), A]\|$ and only do further computations on

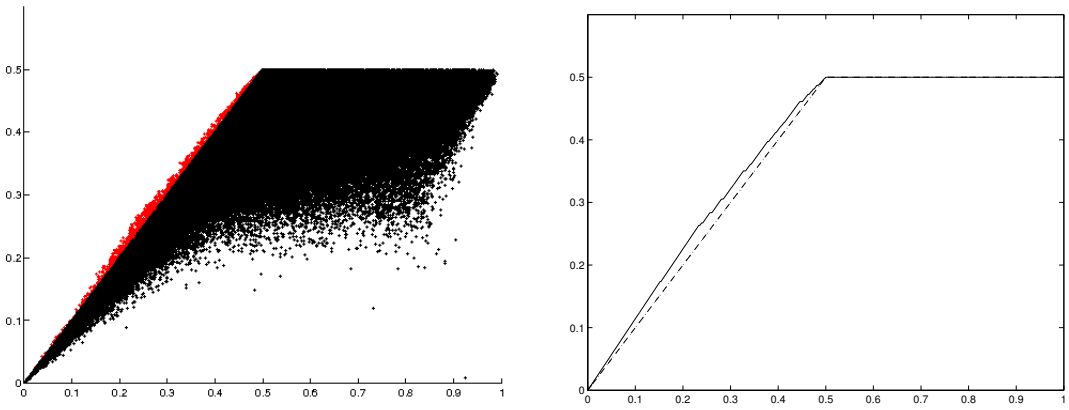

FIGURE 8.2. $f(x) = |x - \frac{1}{2}|$ on $[0, 1]$ and $n = 4$. Approximately 500,000,000 pairs were tested, with 557,550 pairs computed precisely.

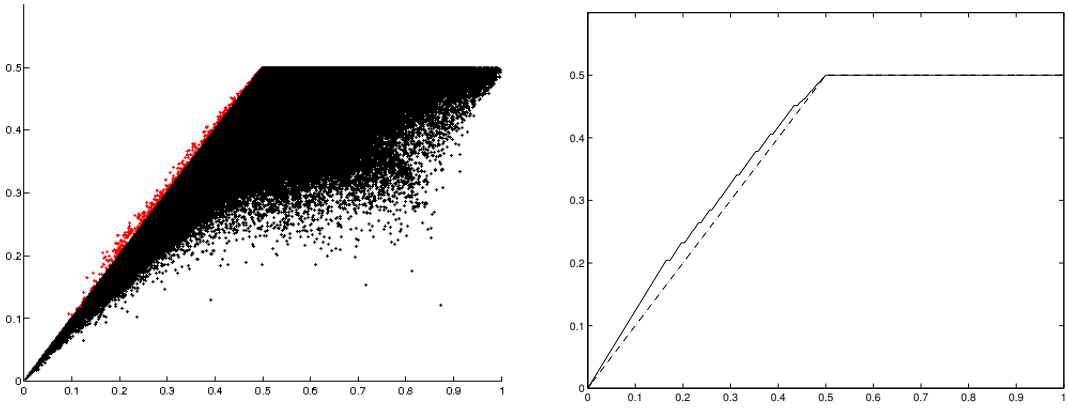

FIGURE 8.3. $f(x) = |x - \frac{1}{2}|$ on $[0, 1]$ and $n = 8$. Approximately 500,000,000 pairs were tested, with 729,329 pairs computed precisely.

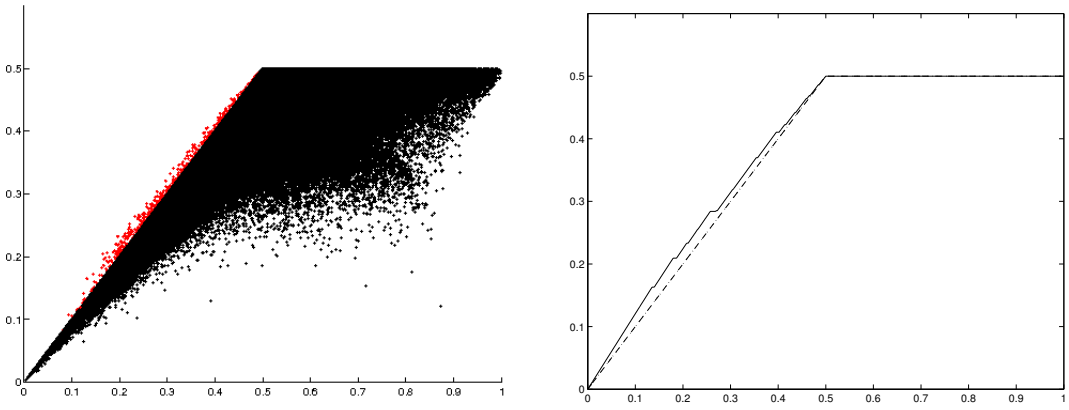

FIGURE 8.4. $f(x) = |x - \frac{1}{2}|$ on $[0, 1]$ and $n = 16$. Approximately 500,000,000 pairs were tested, with 1,048,860 pairs computed precisely.

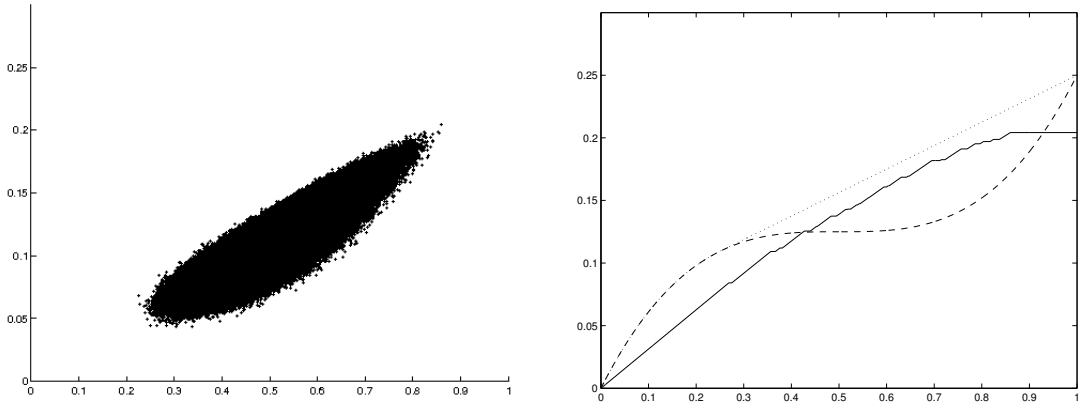

FIGURE 9.1. $f(x) = (x - \frac{1}{2})^3$ on $[0, 1]$ and $n = 16$. Approximately 10,000,000 pairs were tested. The algorithm uses uniform distribution to create the test matrices and all pairs are computed exactly. Time needed on a 32 core machine: 123 minutes.

pairs that are provisionally placing high on the plot compared what has come before. These promising pairs are then adjusted so that $0 \leq X \leq 1$ and $\|A\| = 1$ are as true as is possible within Matlab. Then $\|[X, A]\|$ and $\|[f(X), A]\|$ are computed by slow but precise methods and the point is plotted.

The piecewise linear bounds that Lemma 3.1 provides are then derived and the maximum of all these upper bounds is then displayed.

Since the ad-hoc methods are not really justified by any theory, we do not attempt much of an explanation. We will be posting the code on the Arxiv, accompanying a preliminary version of this article.

The essence of the method is as follows. We start with two commuting real symmetric matrices X and A. The fact that real matrices are sufficient follow from the embedding of $\mathbb{C}$ into $\mathbb{R}$. We force them to commute by making them diagonal. A basis change argument validates this.

Next we perturb A by a "random" real symmetric matrix. Here we rely on Lin's theorem to know that all almost commuting hermitian matrices can be found by perturbing commuting pairs. The generation of the random displacement involves a distribution that is very far from uniform. This was needed to avoid the "expected value" problem mentioned above. Finally, the norm of the displacement is calculated and then the displacement is scaled by a random choice that emphasizes smaller displacements. This step was taken since our rigorous upper-bounds are less informative for smaller δ.

We emphasize again that while we cannot rigorously explain our choice of random method or our pre-screening by norm approximations, all of the points plotted are computed very precisely.

We can illustrate the need for the custom distributions easily. Figure 9.1 shows a calculation done for $f(x) = (x - \frac{1}{2})^3$ with uniform distribution used for generating the displacement. This is to be contrasted with the data in Figure 9.2 where a fast pre-screening is done, and data in Figure 9.3 where our non-uniform distribution is used. Finally Figure 9.4 shows the use of the non-uniform distribution and the pre-screening. Note the timing data, that shows how much time was needed to generate these plots and the time sized by the pre-screening.

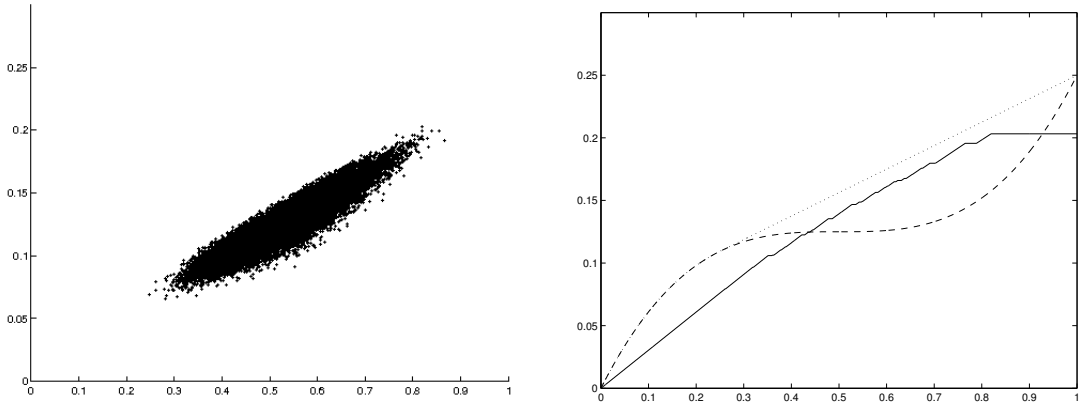

FIGURE 9.2. $f(x) = (x - \frac{1}{2})^3$ on $[0, 1]$ and $n = 16$. Approximately 10,000,000 pairs were tested. The algorithm uses uniform distribution to create the test matrices, but only pairs where the estimated norm predicts a point that is high are computed exactly and plotted. Time needed on a 32 core machine: 18 minutes.

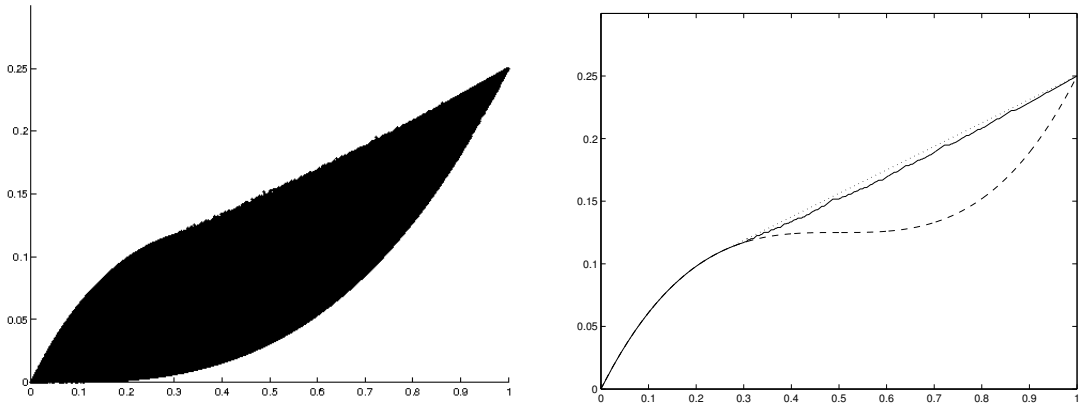

FIGURE 9.3. $f(x) = (x - \frac{1}{2})^3$ on $[0, 1]$ and $n = 16$. Approximately 10,000,000 pairs were tested. The algorithm uses a very non-uniform, and all pairs are computed exactly. Time needed on a 32 core machine: 124 minutes.

10. Acknowledgements

This work was partially supported by a grant from the Simons Foundation (208723 to Loring) and utilized much computing time the Center for Advance Research Computing at the University of New Mexico.

References

[1] A. B. Aleksandrov and V. V. Peller, *Operator Hölder-Zygmund functions*, Adv. Math. 224:3 (2010) pp. 910–966.

[2] A. B. Aleksandrov and V. V. Peller, *Estimates of operator moduli of continuity*, J. Funct. Anal., 261:10 (2011), pp. 2741–2796.

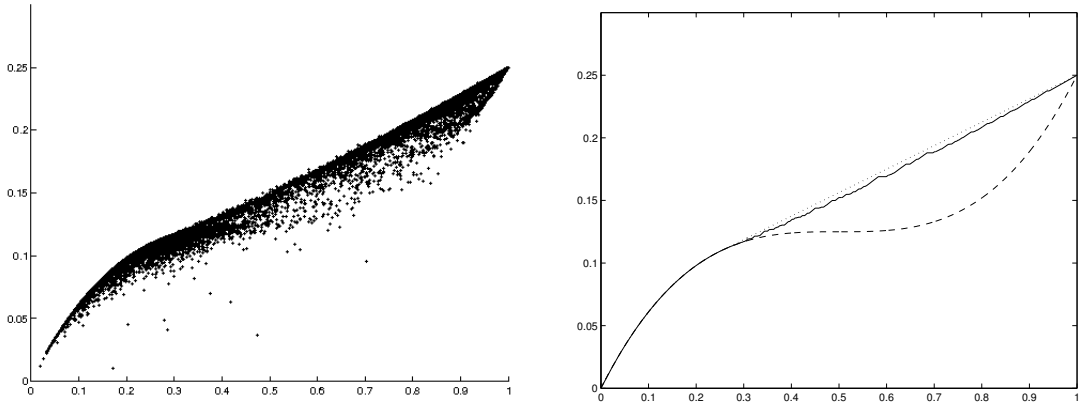

FIGURE 9.4. $f(x) = (x - \frac{1}{2})^3$ on $[0, 1]$ and $n = 16$. Approximately 10,000,000 pairs were tested. The algorithm uses a very non-uniform and non-normal distribution to create the test matrices, but only pairs where the estimated norm predicts a point that is high are computed exactly and plotted. Time needed on a 32 core machine: 19 minutes.

[3] R. Bhatia and F. Kittaneh, *Some inequalities for norms of commutators*, SIAM J. Matrix Anal. Appl., 18 (1997), pp. 258–263.

[4] A. Böttcher and D. Wenzel, *How big can the commutator of two matrices be and how big is it typically?*, Linear Algebra Appl., 403 (2005), pp. 216–228.

[5] K. N. Boyadzhiev, *Norm estimates for commutators of operators*, J. London Math. Soc. (2), 57:3 (1998), pp. 739–745.

[6] S. Eilers and R. Exel *Finite-dimensional representations of the soft torus* Proc. Amer. Math. Soc., 130:3 (2002), pp. 727–731.

[7] R. Exel and T. A. Loring, *Invariants of almost commuting unitaries*, J. Funct. Anal., 95 (1991), pp. 364–376.

[8] M. B. Hastings and T. A. Loring, *Topological insulators and C^*-algebras: Theory and numerical practice*, Ann. Physics, 326 (2011), pp. 1699–1759.

[9] T. Kato, *Continuity of the map $S \mapsto |S|$ for linear operators*, Proc. Japan Acad., 49 (1973), pp. 157–160.

[10] T. A. Loring, *From matrix to operator inequalities*, Canad. Math. Bull., 55:2 (2012) pp. 339–350.

[11] G. K. Pedersen, *The corona construction*, in Operator Theory: Proceedings of the 1988 GPOTS-Wabash Conference (Indianapolis, IN, 1988), vol. 225 of Pitman Res. Notes Math. Ser., Longman Sci. Tech., Harlow, 1990, pp. 49–92.

[12] ——, *A commutator inequality*, in Operator algebras, mathematical physics, and low-dimensional topology (Istanbul, 1991), vol. 5 of Res. Notes Math., A K Peters, Wellesley, MA, 1993, pp. 233–235.

[13] S. Sakai, *Operator Algebras in Dynamical Systems*, in Encyclopedia of Mathematics and its Applications, Vol. 41, Cambridge University Press 1991.

Department of Mathematics and Statistics and the Center for Advanced Research Computing, University of New Mexico, Albuquerque, NM 87131, USA.